Eur. Phys. J. D **5**, 83–88 (1999)

THE EUROPEAN PHYSICAL JOURNAL D

EDP Sciences

Molecular dynamics simulation of C_2H_2 deposition on diamond (001)–(2 × 1) surface

W.J. Zhu[1], Z.Y. Pan[1,2,a], Y.K. Ho[3,1], and Z.Y. Man[1]

[1] State key laboratory for materiel modification by laser, Ion and electron beams, Institute of Modern Physics, Fudan University, Shanghai 200433, P.R. China
[2] Ion beam laboratory, Shanghai Institute of Metallurgy, Chinese Academy of Science, Shanghai 200433, P.R. China
[3] CCAST (world laboratory), P.O. Box 8730, Beijing 100080, P.R. China

Received: 19 May 1998 / Accepted: 26 July 1998

Abstract. We studied the deposition dynamics of C_2H_2 molecules on diamond reconstructed (001)–(2×1) surface by molecular dynamics method using semi-empirical many-body Brenner potential (#2). The chemisorption of C_2H_2 on diamond was found to occur with C_2H_2 bonding directly to the surface radical sites. Six stable chemisorption configurations have been identified. The majority of chemisorption are observed to have two C–C_s bonds between C_2H_2 and the diamond surface. An energy threshold effect for surface reaction between the gas molecule and the surface,which is sensitive to the impinging position of C_2H_2 on the dimerized surface, has been observed. Furthermore the energy transfer during the collision has been analyzed.

PACS. 79.20.Rf Atomic, molecular, and ion beam impact and interactions with surfaces – 61.20.Ja Computer simulation of liquid structure – 81.15.Gh Chemical vapor deposition (including plasma-enhanced CVD, MOCVD, etc.)

1 Introduction

Diamond has an unique combination of physical, chemical, electrical and optical properties which make it potentially attractive for a large number of important industrial applications. For example, its extreme hardness and wear resistance make it ideal for coating tools. Its transparency, insulating properties, radiation hardness and excellent thermal conductivity make it a good candidate for future application in circuit packaging, high power, electro-optic, semiconductor devices and optical devices [1,2]. These applications are expanded due to the successful synthesis of stable diamond thin films by the low pressure chemical vapor deposition (CVD), such as hot filament CVD, microwave plasma-assisted CVD, DC arc plasma jet and Flame deposition [3–6]. During the chemical vapor deposition process of diamond, the reaction of hydrocarbon radical chemisorption on diamond surface is critical in diamond synthesis. This reaction mechanism was studied both experimentally and theoretically [7–11]. Methyl radical (CH_3) and Acetylene (C_2H_2) were considered to be key primary species during diamond synthesis [12–16]. Michale Frenkach proposed a pathway of diamond growth *via* C_2H_2 and CH_3 adsorption [17]. Alfonso [18] calculated the binding energy of C_2H_2 adsorption at trough site and bridge site of diamond (100) surface by molecular dynamics method. Peploski [11] claimed that the reaction of hydrocarbon radical on diamond surface can be determined by dynamics process and used that to be simulate the chemisorption of C_2H_2 on diamond (111). The result showed that the chemisorption configuration with two σ bonds between C_2H_2 and the diamond surface was the most stable one. Therefore the study of the interaction dynamics between C_2H_2 molecule and diamond (001) surface would be interesting but it has not been reported so far. Moreover, the reaction dynamics of gas molecules on surface affects the efficiency and quality of thin film fabrication under low pressure chemical vapor deposition condition. So the study of interaction dynamics of C_2H_2 on diamond (001) surface should shed some light on the mechanism of diamond synthesis.

In this article we investigated the microscopic interaction dynamics of low energy C_2H_2 on the diamond (001)–(2×1) surfaces of atomic level using molecular dynamics method. The relationship between molecule-surface interaction dynamics and the molecule chemisorption behavior on surface was studied. We also explored possible C_2H_2 chemisorption configurations and the dependence of their formation on the incident energy, impinging position, and surface structure. The calculation model is introduced in Section 2. Computational results and discussion are given in Section 3.

[a] e-mail: hoyk@fudan.ac.cn

2 Computational model

In order to describe the interaction between C_2H_2 and diamond surface involved in C–H system, we employed the semi-empirical many-body Brenner (#2) potential [19], which was developed from Tersoff potential [20] with bond order function correction. The binding energy for this hydrocarbon potential is given as a sum over bonds by:

$$E_b = \frac{1}{2}\sum_i \sum_{j\neq i} \left[V_R(r_{ij}) - \bar{B}_{ij} V_A(r_{ij})\right] \quad (1)$$

where

$$V_R(r_{ij}) = f_{ij}(r_{ij}) D_{ij}^{(e)}/(S_{ij}-1) e^{-\sqrt{2S_{ij}}\beta_{ij}(r_{ij}-R_{ij}^{(e)})} \quad (2)$$

$$V_A(r_{ij}) = f_{ij}(r_{ij}) D_{ij}^{(e)} S_{ij}/(S_{ij}-1) e^{-\sqrt{2S_{ij}}\beta_{ij}(r_{ij}-R_{ij}^{(e)})} \quad (3)$$

$$\bar{B}_{ij} = (B_{ij}+B_{ji})/2 + F_{ij}(N_i^{(t)}, N_j^{(t)}, N_{ij}^{conj})/2. \quad (4)$$

In the above equations, E_b is the binding energy for the system, $V_R(r_{ij})$ and $V_A(r_{ij})$ are the repulsive and attractive potential between atom i and atom j. $\bar{B}_{ij}$ is the bond order function which corrects for an inherent overbinding of radicals and includes nonlocal effects. Atomization energies computed using this potential for 12 alkanes, 13 alkenes, 4 alkynes, 7 aromatics, and 12 radicals are found to be in good agreement with experimental values within less than 1.5%. The calculated lattice structure parameters of diamond and graphite are also in good agreement with experiments. The covalent bond breaking and forming in various hydrocarbon molecules are known to be well-described by this potential [19]. Moreover, the C–C bond length and C–H bond length involved in C_2H_2 molecule are calculated, the values 1.28 Å and 1.07 Å are consistent with the measured values of 1.21 Å and 1.08 Å respectively. Lattice parameters, such as C_s–C_s bond length (subscript s denotes surface carbon atom) and dimer length of the reconstructed diamond (001) surface, are same as those in Brenner's work [19]. Following these preparatory calculations we went on to simulate the interaction between energetic C_2H_2 molecules and diamond (001) reconstructed surfaces.

In the present study, the diamond surface is composed of 12 layers with 64 atoms per layer. The bottom two layers are held fixed during the simulation. The motion of atoms in top two layers is determined by the force produced by the Brenner potential. The velocity scaling method [21] is applied to the middle eight layers in order to maintain the substrate temperature at a constant magnitude of 300 K. Periodic boundary conditions are employed in the two directions paralleled to the surface. The diamond (001)–(2×1) surface structure is shown in Figure 1. Before the deposition begin the system has been relaxed in 300 K thermal bath for 3 ps allowing it to approach a thermal equilibrium state. The incident direction of C_2H_2 molecules is perpendicular to the diamond surface. The orientation of C_2H_2 molecule is shown in Figure 2. The incident molecules are assumed to be rotational "and vibrational" cold. The incident energy is in the range of 1 eV $\leq E_{kin} \leq$ 15 eV. The incident molecule is initially located at 3 Å above the diamond surface where the interactions between the molecule and the substrate atoms are negligible. The trajectories are determined by integrating the motion equations according to the Leap-Frog algorithm [22]. The integrating calculation lasts for around 3 ps, after that the configurations appear to be stable.

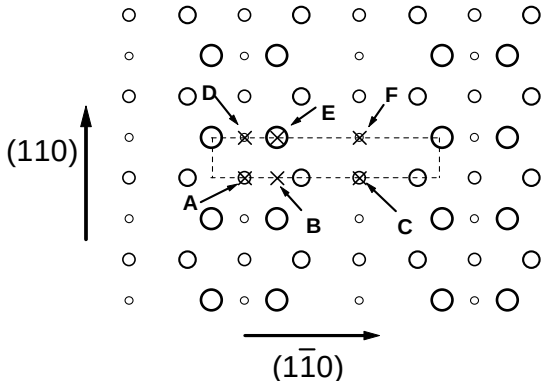

Fig. 1. The top view of diamond (001)–(2×1)reconstructed surface. The six selected impinging positions A, B, C, D, E and F are represented by "×" symbol. The dash-line enclosed area is the impinging area.

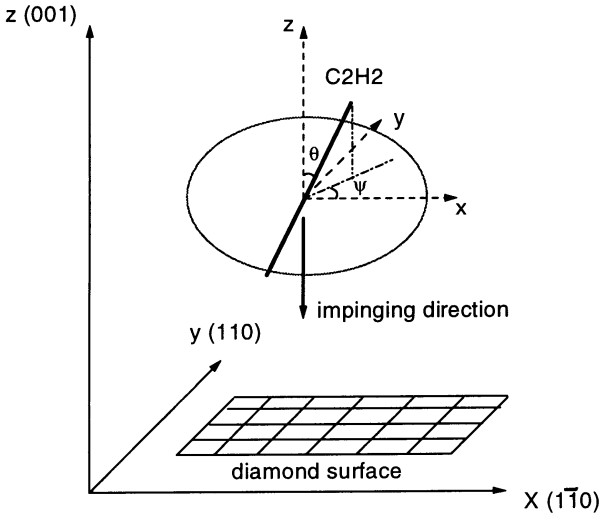

Fig. 2. Geometric representation of C_2H_2 impinging on diamond surface. θ and ψ are the polar and azimuthal angle of the C_2H_2 molecule relative to the impinging direction along the minus z axis.

3 Result and discussion

To study possible chemisorption configurations of C_2H_2 molecule on diamond surfaces it is important to understand the behavior in the initial stage of diamond film fabrication. Two hundred examples of C_2H_2 molecules

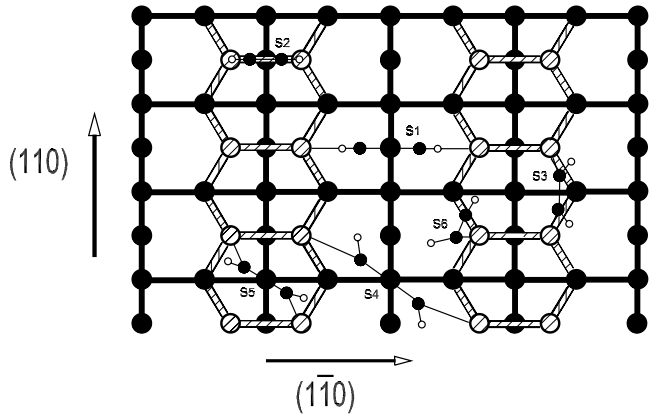

Fig. 3. Top view of the six possible chemisorption configurations shown as S1, S2, S3, S4, S5 and S6 on diamond (001)–(2×1) surface. The hatched circles represent the surface dimers. The big solid circles represent the subsurface atoms. The small solid circles represent the carbon atoms of C_2H_2. The hollow circles represent the hydrogen atoms of C_2H_2. The broad solid lines represent the bonds between the subsurface atoms. The hatched lines represent the bonds between the surface dimer atoms and the subsurface atoms. The thin solid lines represent the bonds between the atoms of C_2H_2 and the surface dimer atoms.

impinging on diamond reconstructed (001) surface were studied using MD simulation technique with the above mentioned interaction potential. The impinging position was randomly selected within the area enclosed by dashed-line showed in Figure 1. The orientation of C_2H_2 was also randomly chosen. The incident energy was fixed at 10 eV. We found that in about 95% of the chemisorption events, the C_2H_2 molecules form two C–C_s bonds with the diamond surface. A total of six chemisorption configurations were observed as shown in Figure 3. Two of these, the bridge and trough sites, were computed previously [18]. The other four are first presented here. We also calculated the binding energy of these six chemisorption structures by the steepest decent method and the results are given in Table 1. The surface structure parameters before and after chemisorption are also listed in Table 1. It can be seen that the surface atom activation varies with the reconstructed surface structure. In the case of S1 structure, C_2H_2 molecule is adsorbed on two adjacent dimer sites in the same row across a trough forming two C–C_s bonds. The S1 structure has the largest binding energy and it's the most stable chemisorption configuration. Since the distance between two adsorption sites in S1 structure is separated by a trough, it is difficult for the S1 structure to occur during deposition process. In S2 structure, the C_2H_2 molecule is adsorbed on the bridge sites of the same dimer forming two C–C_s bonds. The feature of S3 structure shows that the C_2H_2 molecule forms two C–C_s bonds on the same side of two dimer along (110) direction. The binding energies of the S2 structure and the S3 structure are smaller than that of the S1 structure, but the distances between the two sites in S2 and in S3 structure favor their corresponding kind of chemisorption configuration to occur. Therefore those two chemisorption structures may play an important role in diamond synthesis. The S4 structure features two C–C_s bonds on two dimers from different rows across a trough. The S5 structure is characterized by C_2H_2 lying on the same dimer column with two C–C_s bonds on two dimer sites from different rows. The S6 structure only involves one C–C_s bond between the C_2H_2 molecule and surface dimer, which is the most unstable chemisorption structure. This viewpoint is confirmed also by the binding energy calculation which shows that S6 structure is least affected in diamond fabrication.

Table 1. The binding energy and the structure parameters of the six chemisorption structures. BE is binding energy. r(C–C_s) is the single bond formed between C_2H_2 molecule and the surface carbon atom. r(C–C) is the bond length between the two carbon atoms of C_2H_2 after chemisorption. r_0(C_s–C_s) is the distance between two reactive sites before chemisorption. r(C_s–C_s) is the distance between two reactive sites after chemisorption.

Chemisorption Structure	S1	S2	S3	S4	S5	S6
BE (eV)	3.57	3.22	2.95	1.97	2.06	0.33
r(C–C_s) (Å)	1.51	1.55	1.51	1.55	1.54	1.50
r(C–C) (Å)	1.38	1.42	1.39	1.41	1.40	1.40
r_0(C_s-C_s) (Å)	3.60	1.43	2.52	4.39	2.90	-
r(C_s–C_s) (Å)	3.07	1.66	2.42	3.66	2.77	-

In order to study the effect of varying incident energy, we explored the interaction dynamics of C_2H_2 impinging on diamond surfaces for the six fixed impinging positions as shown in Figure 1. The incident energy was changed with 1 eV increment from 1 eV to 15 eV and the molecular spatial orientation is chosen to be $\theta = 0°$ (see Fig. 2). The simulation results show that there exist an energy threshold for C_2H_2 chemisorption to occur. When the incident energy is lower than the threshold, the molecule will rebound from the surface. Also, the threshold value is sensitive to the incident position. This is because for a chemisorption to occur, some energy is needed to break the C–C triple bond of C_2H_2 molecule and the surface dimer bonds, so that new C–C_s bonds can be formed. Since the energy transfer process depends on the local surface structure. Therefore incident energy thresholds are different for chemisorption of C_2H_2 at different impinging positions. The observed threshold values for different impinging position are shown in Figure 4.

For the case of impinging position A, there is no chemisorption observed even at the incident energy up to 15 eV. Figure 5 shows the kinetic energy and mass center height of C_2H_2 as a function of time at incident energy 10 eV for impinging position A. At the beginning of the interaction (at $t_1 = 20$ fs), only one hydrogen atom of the C_2H_2 molecule interacts with the surface carbon atoms. A part of the incident kinetic energy is transferred to the potential energy and kinetic energy of the surface atoms

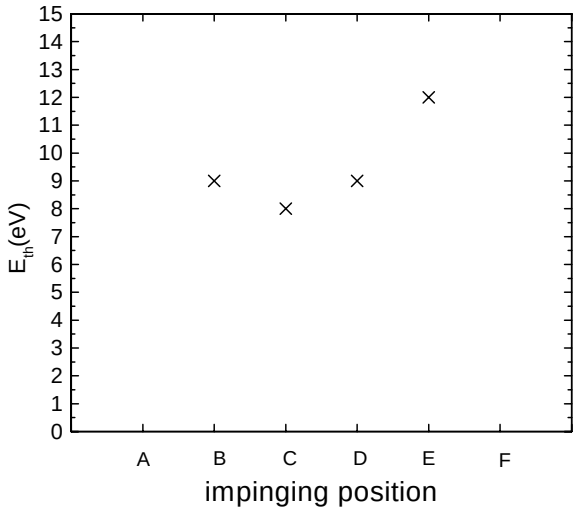

Fig. 4. The energy thresholds of chemisorption for the impinging events B, C, D, E (see Fig. 1). There is no chemisorption to be observed for the impinging events A, F (see Fig. 1). The incident energy is in the range of 1 eV $\leq E_{kin} \leq$ 15 eV. The incident direction is normal to the diamond surface and the orientation of the C_2H_2 is chosen to be $\theta = 0°$ (see Fig. 2).

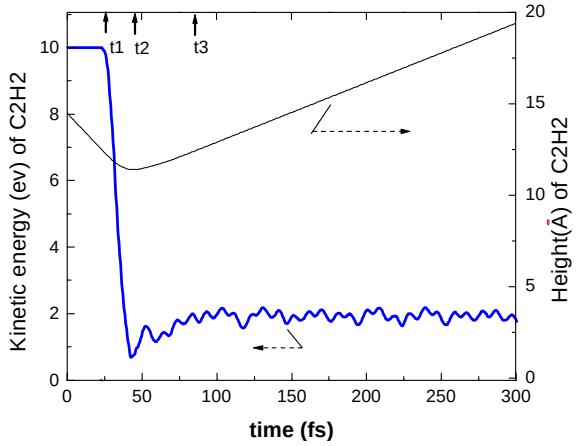

Fig. 5. Time evolutions of the kinetic energy and height of the of C_2H_2 mass center for the incident event with impinging position A shown in Figure 1. The molecule is incident normally onto the surface with initial energy 10 eV. The height of the surface is $\simeq$ 9.6 Å while the height of the diamond slab bottom at 0 Å.

through the interaction between this hydrogen atom and the surface atoms, and to the compression of C–H bond of C_2H_2. This hydrogen atom locates at the center of two dimers and interacts with four carbon atoms symmetrically. Therefore, the linear molecule is difficult to be folded. It prevents the carbon atoms of C_2H_2 to come close to and interact with the surface atoms. Twenty femtoseconds later (t_2 = 40 fs), C_2H_2 molecule losses about 97% of its initial kinetic energy. H–C–C bond angle only folds to 153°. At this moment, one carbon atom of C_2H_2 begins to interact with the surface atoms, but the kinetic energy left is not enough to make this carbon atom of C_2H_2 get closer to the surface atoms. After that the deformation of the substrate relaxes and the H–C bond of C_2H_2 stretches, transferring a part of surface potential energy into the kinetic energy of C_2H_2. At time t_3 = 80 fs, the C_2H_2 molecule rebounds from the diamond surface with about 1.9 eV kinetic energy.

For the case of impinging position B, if the incident energy is less than 9 eV, the C_2H_2 molecule rebounds from the surface. Otherwise it will be adsorbed. Figure 6 shows the snapshots of C_2H_2 molecule with 10 eV incident energy interacting with surface atoms, whereas Figure 7 shows the kinetic energy of C_2H_2 and the system potential energy change as a function of time of the same trajectory. At t_1 = 20 fs, the C_2H_2 molecule begins to interact with the surface atoms and the energy transfer process is the same as that for position A. However, in this case the surface carbon atoms interacting with the C_2H_2 molecule are asymmetric relative to its orientation causing the H–C–C bond angle to fold rapidly. At time t_2 = 38 fs, the H–C–C bond angle folds to 95° and one C atom of C_2H_2 begins to interact strongly with the surface atoms. At this moment, the kinetic energy of C_2H_2 losses only about 50%, so that the C atom of C_2H_2 can reach the surface atoms more closely. Seventeen femto-seconds later, the distance between the C atom and its nearest surface atom becomes 1.5 Å, which means the C atom falls into a C–C_s bond potential well. The newly formed C–C_s bond oscillates within the range of 1.42 Å to 1.67 Å, resulting in stretching the dimer bond from 1.42 Å to 1.56 Å as well as the C–C bond length of C_2H_2 to 1.40 Å. The H–C–C bond angle fluctuates around 120°. The changes of those parameters mean that recrystallization happens. Because of the steric repulsive force, another H–C–C bond angle folds to 136° and makes another C atom of C_2H_2 to become a dangled bond, which has strong attractiveness. Then this C atom turns around the newly formed C–C_s bond. And at the time t_3 = 267 fs, it interacts with a surface atom, forming a S4 chemisorption structure (see Fig. 3) as its intermediate process. This atom will leave the potential well since it has enough kinetic energy. Thirty femto-seconds later, the atom falls into another C–C_s bond potential well. Then a more stable chemisorption structure S3 (see Fig. 3) is formed at the time t_4 = 360 fs. After that, the kinetic energy of C_2H_2 decreases with relaxation and thermalization of the substrate surface atoms. Figure 7 shows that after the S3 chemisorption structure is formed, the system potential energy continue to decrease. It's clear that the chemisorption process is an exothermal reaction and the thermal energy is dissipated by the diamond lattice vibrations.

As shown in Figure 4, threshold energy for chemisorption is observed in the energy range chosen for the impinging position C, D and E, but not for the case of F. This fact can be deduced by looking at the local atomic configuration of the impinging positions.

With regard to the effect of C_2H_2's orientation to chemisorption, we study the case of impinging position A with various orientation variables θ and ψ in Figure 2. In the case of θ = 45° and ψ = 0°, no chemisorption is observed in the incident energy range (1 − 15 eV).

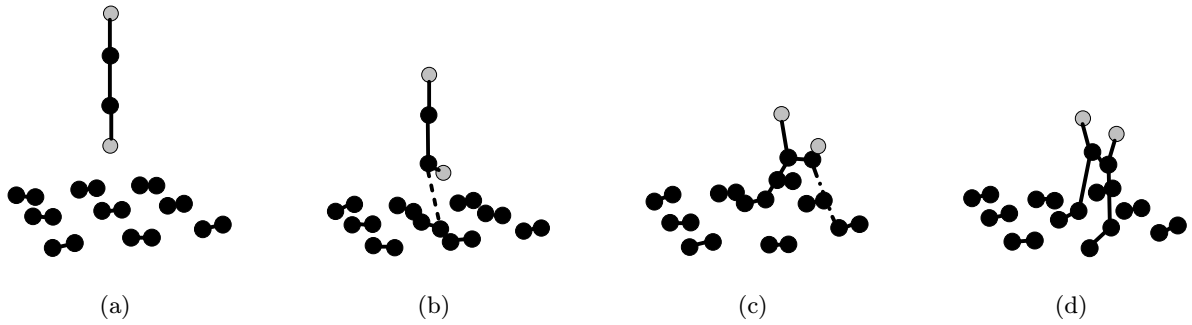

Fig. 6. Snapshots of the C_2H_2 chemisorption for the impinging event B (see Fig. 1). The molecule is incident normally onto the surface with initial energy 10 eV. (a) $t_1 = 20$ fs, (b) $t_2 = 38$ fs, (c) $t_3 = 267$ fs, (d) $t_4 = 360$ fs. The dashed-lines are the main interactions. The solid lines show the chemical bonds formed.

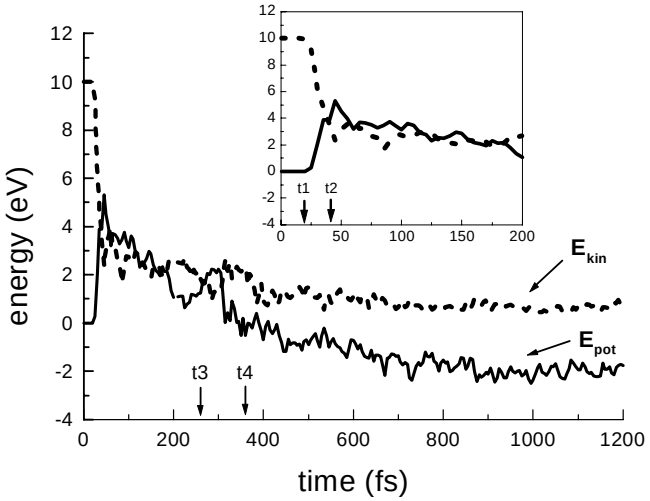

Fig. 7. Time evolutions of the kinetic energy of C_2H_2 mass center and the total potential energy change of the system for impinging event B (see Fig. 1). The solid-lines show the total potential energy change of the system. E_{pot} is set to zero at $t = 0$. The dashed-lines show the kinetic energy of C_2H_2 mass center. The inset shows the details of evolution during the first 200 fs.

When $\theta = 90°$ and $\psi = 0°$, the molecule is parallel to the surface, chemisorption is observed for incident energies above 7 eV. Another example is $\theta = 45°$ and $\psi = 90°$, the energy threshold for chemisorption is found to be 9 eV. Fixing $\psi = 90°$ and $\theta = 90°$, the energy threshold for chemisorption is 6 eV. In one word, chemisorption is sensitive to the impinging position, incident energy, and the molecular orientation.

4 Conclusion

We studied by using molecular dynamics method impinging dynamic of energetic C_2H_2 molecule on diamond (001)–(2×1) surface at room temperature with the specific intention on observing the chemisorption process, which is regarded as the initial stage of the recrystallization of the molecules on the substrate surface. Our results can be summarized as follows.

1. Six types of chemisorption configurations have been observed. Two of those appeared in previous publication [18], the other four are reported for the first time here. The characteristic of those chemisorption configurations are shown in Figure 3 and listed in Table 1. The majority of those chemisorption configurations are observed to have two C–C_s bonds between C_2H_2 and the diamond surface.
2. Upon impacting, the incident translational energy of C_2H_2 is transferred to the internal energies of both C_2H_2 and the surface. These energies induce the breaking of the molecular C–C triple bond, the opening of surface dimers, and the folding of the molecule. Those are the main factors in the formation of various chemisorption configurations, especially the stable ones.
3. We have observed energy threshold effect for chemisorption. That is, with fixed orientation of C_2H_2 and impinging position, chemisorption can occur only when the incident energy $E_{in} \geq E_{th}$, the threshold energy.
4. The magnitude of E_{th} has been found to be sensitive to the spatial orientation of C_2H_2 and the impinging position, as shown in Figure 4.

This article is limited to the study of a single molecule interacting with diamond surface, the possible chemisorption configurations and their dynamics processes. Many questions such as the role played by the hydrogen atoms for the CVD process, multiple C_2H_2 molecules interaction with each other and diamond surface are still open for further discussion. We plan to study these questions in the near future.

This work has been supported partly by the National Natural Science Foundation of China, the Doctorate Research Foundation of the Eduction Commission of China. The authors wish to thank Prof. C.M. Fou for carefully reading of this manuscipt and enlightening discussion.

References

1. J.C. Angus, C.C. Hayman, Science **241**, 913 (1988).
2. D. Tither, W. Ahmed, E. Ahmed, J. Matt. Sci. **32**, 1931 (1997).
3. T. Kawatand, K. Kondo, Jpn J. Appl. Phys. **26**, 1429 (1987).
4. P. Reinke, P. Kania, P. Oelhafen, Thin Solid Film **270**, 124 (1995).
5. K. Kurihara, K. Sasaki, M. Kawarada, N. Koshino, Appl. Phys. Lett. **52**, 437 (1988).
6. M.A. Cappelliand, P.H. Paul., J. Appl. Phys. **67**, 2596 (1990).
7. B. Ruf, F. Behrendt, O. Deutschmann, J. Warmatz, Surf. Sci. **352-354**, 602 (1996).
8. D.R. Alfonso, S.E. Ulloa, Phys. Rev. B **48**, 12235 (1993).
9. B.D. Thoms, J.N. Russell Jr., P.E. Pehrsson, J.E. Butler, J. Chem. Phys. **100**, 8425 (1994).
10. S. Kato, H. Hu, Surf. Sci. **357-358**, 891 (1996).
11. J. Peploski, D.L. Thompson, L.M. Raff, J. Phys. Chem. **96**, 8539 (1992).
12. M. Frenkach, K.E. Spear, J. Mater. Res. **3**, 133 (1988).
13. D.G. Goodwin, G.G. Gavillet, J. Appl. Phys. **68**, 6393 (1990).
14. S.J. Harris, A.M. Weiner, T.A. Perry, Appl. Phys. Lett. **53**, 1605 (1988).
15. D. Huang, J. Phys. Chem. **92**, 6379 (1988).
16. M. Tsuda, M. Nakajima, S. Oikawa, J. Am. Chem. Soc. **108**, 5780 (1986).
17. M. Frenklach, J. Chem. Phys. **97**, 5794 (1992).
18. D.R. Alfonso, S.E. Ulloa, D.W. Brenner, Phys. Rev. B **49**, 4948 (1994).
19. D.W. Brenner, Phys. Rev. B **42**, 9458 (1990).
20. J. Tersoff, Phys. Rev. B **37**, 6991 (1988).
21. D. Brown, J.H.R. Clarke, Mol. Phys. **51**, 1243 (1984).
22. L. Verlet, Phys. Rev. A **159**, 98 (1967).